

SYNCHRONOUS LASER-MICROWAVE NETWORK FOR ATTOSECOND-RESOLUTION PHOTON SCIENCE

K. Şafak[†], F. X. Kärtner¹, A. Kalaydzhyan, O.D. Mücke, W. Wang, M. Xin¹
CFEL - DESY, Hamburg, Germany

M. Y. Peng, MIT, Cambridge, Massachusetts, USA

¹also at MIT, Cambridge, Massachusetts, USA

Abstract

Next-generation photon-science facilities such as X-ray free-electron lasers and intense-laser beamline centers are emerging worldwide with the goal of generating sub-fs X-ray pulses with unprecedented brightness to capture ultra-fast chemical and physical phenomena with sub-atomic spatiotemporal resolution. A major obstacle preventing this long-standing scientific dream to come true is a high precision timing distribution system synchronizing various microwave and optical sub-sources across multi-km distances. Here, we present, for the first time, a synchronous laser-microwave network providing a timing precision in the attosecond regime. By developing new ultra-fast timing detectors and carefully balancing optical fiber nonlinearities, we achieve timing stabilization of a 4.7-km fiber link network with 580-attosecond precision over 52 h. Furthermore, we realize a complete laser-microwave network incorporating two mode-locked lasers and one microwave source with total 950-attosecond jitter integrated from 1 μ s to 18 h.

INTRODUCTION

Drift-free and long-distance transfer of time and frequency standards provides high-temporal resolution for ambitious large-scale, scientific explorations. To name a few: sensitive imaging of low temperature black bodies using multi telescope arrays [1]; gravitational deflection measurements of radio waves using very-long-baseline interferometry [2]; synchrotron light sources [3], gravitational-wave detection using large laser interferometers [4], and next-generation photon science facilities such as X-ray free-electron lasers (XFELs) [5] and laser-based attoscience centers [6]. Among these, XFELs and attoscience centers demand the most challenging synchronization requirements with sub-femtosecond precision to generate ultrashort X-ray pulses for the benefit of creating super microscopes with subatomic spatiotemporal resolution [7]. To achieve this, it is necessary to develop an attosecond-precision timing distribution system (TDS) to synchronize various microwave and optical sub-sources across the km-scale facilities to deliver the timing stability required for seeded FEL operation and attosecond pump-probe measurements.

So far, there has been no TDS meeting this strict requirement. Although research in attosecond X-ray pulse generation has progressed rapidly in the past few years

[8], sub-atomic-level measurements cannot be performed due to the lack of a high-precision timing control. Hence, low temporal precision provided by the current synchronization systems remains to be a major obstacle from realizing attosecond hard-X-ray photon-science facilities.

There are two general synchronization schemes reported so far. The first scheme uses microwave signal distribution via amplitude modulation of a continuous-wave laser and employs electronic phase-locking techniques to synchronize various microwave and pulsed laser sources [9]. However, this technique cannot deliver better than \sim 100-fs RMS jitter across the facility [10] due to low phase discrimination with microwave mixers and high noise floor at photodetection. The second scheme [11], which is further developed in this paper, uses ultralow-noise pulses generated by a mode-locked laser as its timing signal to synchronize optical and microwave sources using balanced optical cross correlators (BOCs) [12,13] and balanced optical-microwave phase detectors (BOMPDs) [14,15], respectively. While this pulsed scheme has breached the 10-fs precision level [15-18], realization of sub-femtosecond precision requires further development of the timing detectors (i.e., BOCs and BOMPDs) and deep physical understanding of optical pulses shaping in fiber transmission.

This paper starts with the recent developments achieved in timing detection schemes, and then demonstrates the synchronous laser-microwave network delivering attosecond precision.

TIMING DETECTORS

The primary elements to realize a high precision TDS are the timing detectors as they dictate the smallest timing errors to be detected by the system.

Polarization-noise-suppression in SH-BOCs

Second-harmonic BOC (SH-BOC) (see Figure 1(a)) operating with 1550-nm input pulses is the most widely used timing detector in our system employed to stabilize the transmission delays of our fiber based timing links.

In this SH-BOC scheme, a polarization beam splitter (PBS) spatially combines two orthogonally polarized pulse trains at 1550-nm central wavelength. The input pulses travel in a double-pass configuration inside a periodically poled potassium titanyl phosphate (PPKTP) crystal. The end facet of the crystal has a dichroic coating (DC), which is highly reflective for 1550 nm and anti-reflective for 775 nm wavelength. In this way, the SH pulse generated during the forward pass of the fundamen-

[†] kemal.shafak@desy.de

tal harmonics is separated. The dichroic beam splitter (DBS) on the reverse pass is highly reflective for 775 nm at 45° incident and splits the other second-harmonic pulse from the fundamentals. Finally, a balanced photo detector (BPD) converts the timing error between the input pulses into a voltage signal by detecting the power difference in the generated SH light.

Ideal SH generation for BOC is achieved when the polarization states of the input pulses are perfectly orthogonal to each other. Since all optical components have finite polarization extinction ratios in reality, some portion of the optical power is always projected along the undesired polarization axes of the SH-BOC (see Figure 1(b)). These undesired pulses cause a background noise and make it impossible to lock the system at the zero crossing, i.e., zero AM-to-PM conversion point of the SH-BOC. We are able to remove this noise from our detection using a highly birefringent crystal before the SH-BOC as shown in Figure 1(c). The large birefringence temporally separates the undesired polarization components of the input pulses (i.e., E_{1y} and E_{2x}) so that only the desired ones (i.e., E_{1x} and E_{2y}) can generate SH light. When employed in a TDS, the polarization-noise-suppressed BOC (PNS-BOC) will yield higher signal-to-noise ratio (SNR) and improve the long-term timing stability by removing the background intensity fluctuations of the undesired polarization components.

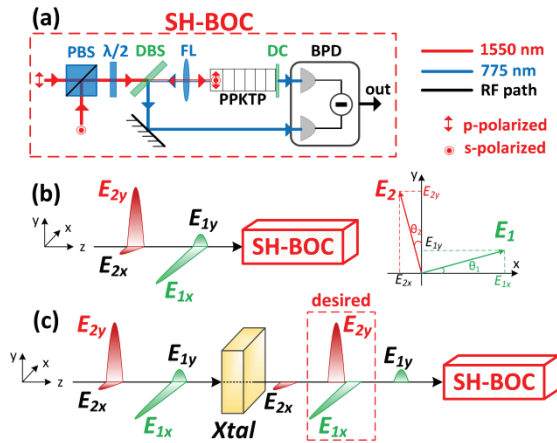


Figure 1: (a) Schematic of type-II second-harmonic BOC for input pulses at 1550 nm. (b) E_1 and E_2 have finite polarization extinction ratios projecting E_{1y} and E_{2x} as noise sources on the opposite principle axes of the type-II crystal. (c) A highly birefringent crystal (Xtal) can avoid this situation by temporally separating the undesired polarization components.

Free-space Coupled BOMPDs

Since XFELs employ many optical and microwave sources in a synchronous operation to generate their radiation, a TDS must also utilize an efficient optical-to-microwave timing detector. To avoid the disadvantages of direct photodetection (e.g., high detection noise floor and excess AM-to-PM conversion) we employ BOMPDs in our TDS, which is an optoelectronic phase-locking tech-

nique converting the phase error between an optical pulse train and a microwave into an intensity modulation of the optical signal [14]. Previous designs of the BOMPD have achieved promising local synchronization results with ~1-fs precision in short time scales (below 1 s) [15]. Nonetheless, they suffer from long-term timing drifts and locking-volatilities due to their vulnerability against environmental changes.

To improve the long-term stability, we have developed free-space coupled BOMPD (FSC-BOMPD) as shown in Figure 2. Key improvements in this BOMPD architecture are as follows. First, free-space optical components are used for the optical beam distribution to the bias, reference and signal paths. Total fiber length of the SGI is spliced to be as short as possible. Compared with the fiber-coupled approach [14,15], free-space optics effectively reduces the long-term drifts caused by the environment. Second, high-frequency operation (13 GHz) at the bias path ensures unidirectional phase modulation in the phase modulator. Since the counter-clockwise pulses do not accumulate phase in the modulator anymore, the SGI becomes repetition rate independent and is more robust against unequal path lengths and environmental fluctuations. Third, down-mixing of the detected SGI output is performed at the lowest frequency possible to maximize SNR at photodetection and to minimize thermally induced phase changes in the reference path. Fourth, free-space delay stages are employed to adjust the relative time delay between the BOMPD paths, which allow precise phase tuning without backlash, microwave reflection and excess loss when compared to electronic phase shifters. Lastly, an AM-PM suppression ratio of -50 dB is achieved by carefully optimizing AM- and PM-sensitive components in the reference and bias paths.

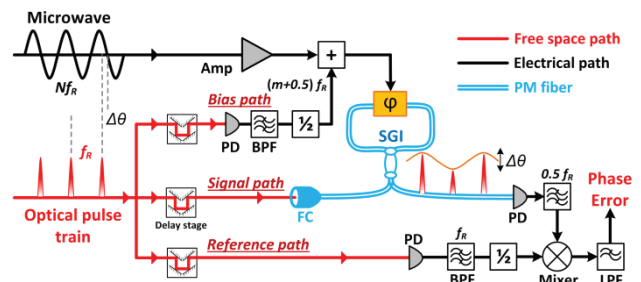


Figure 2: Schematic of free-space-coupled BOMPD. $\Delta\theta$: phase error; PD: photodetector; BPF: bandpass filter; $1/2$: frequency divider; +: diplexer; Amp: electronic amplifier; LPF: lowpass filter; ϕ : phase modulator; SGI: Sagnac-interferometer; FC: fiber collimator.

LASER-MICROWAVE NETWORK

Experimental Setup

Timing precision of an operational TDS is determined by the relative instability between the remote slave optical and microwave oscillators that are synchronized to the master laser by a timing network consisting of many fiber links.

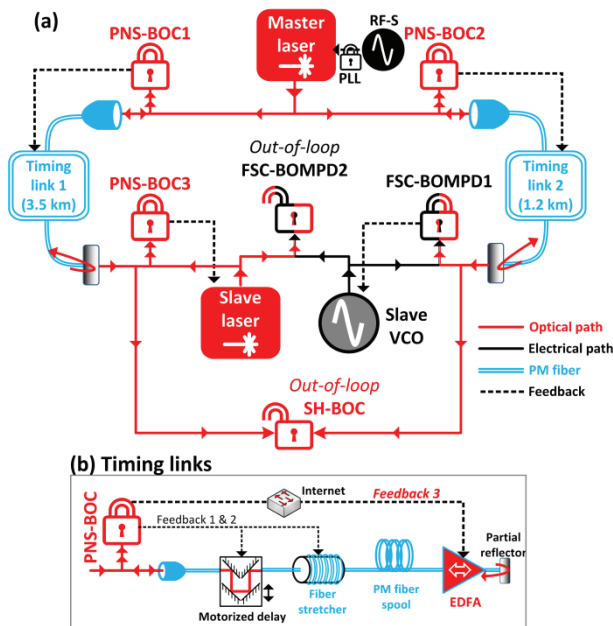


Figure 3: (a) Experimental setup for the laser-microwave network stabilized by PNS-BOCs and FSC-BOMPDPs. (b) Components of the timing links and the applied feedback controls. All timing detectors are symbolized with “lock symbols” shown under their abbreviations. Closed lock refers to an in-loop detector; whereas open lock corresponds to a free-running out-of-loop detector. RF-S: RF synthesizer; PLL: phase-locked loop; PM: polarization maintaining; EDFA: erbium doped fiber amplifier.

We demonstrate such a laser-microwave network experimentally as depicted in Figure 3 incorporating two mode-locked lasers and one microwave source. Our master laser is a mode-locked laser operating at 1554-nm central wavelength with 216.67-MHz repetition rate locked to a RF reference. The output of the master laser is split into two independent timing links with a total length of 4.7 km. Each link consists of a polarization-maintaining (PM) dispersion-compensated fiber spool (1.2 km and 3.5 km long), a PM fiber stretcher, a motorized delay stage and a bi-directional fiber amplifier (EDFA). A partially reflecting mirror at the end of each link reflects 10% of the optical power back to the link input. The reflected pulses are then combined with fresh pulses from the master laser in PNS-BOCs, which measure the propagation delay fluctuations in the links and generate error voltages. Then the fiber stretchers and the motorized delays are activated to compensate for fast jitter and long-term drift, respectively. Our theoretical analysis shows that even in the absence of environmental noise, residual link dispersion and nonlinearities add considerable excess jitter through link transmission and feedback loop [19]. Therefore, residual second- and third-order dispersion of the links are carefully compensated with additional dispersion-compensating fiber to suppress the link-induced Gordon-Haus jitter and to minimize the output pulse durations for high SNR in the BOCs. The link power is adjusted to minimize the nonlinearity-induced jitter as well as to maximize the SNR for BOC locking. Link power

fluctuations can also induce temporal shifts in the pulse center-of-gravity through a composite effect of link residual dispersion and nonlinearity [19]. Therefore, we employ a third feedback control on the pump current of the EDFAs to stabilize the link power fluctuations (Feedback 3 in Figure 3(b)).

The link outputs are used to synchronize a remote laser (e.g., serving as a pump-probe laser at the FEL end station) and a voltage-controlled oscillator (VCO) (e.g., serving as a microwave reference of the FEL Linacs) simultaneously. A third PNS-BOC is built to synchronize the slave laser to timing link 1 output, whereas the slave VCO is locked to timing link 2 output with a FSC-BOMPDP. Finally, timing stability of the link network is measured with an out-of-loop SH-BOC (i.e., by combining the link outputs before remote synchronization), whereas the performance of the complete laser-microwave network is evaluated with an out-of-loop FSC-BOMPDP.

Experimental Results

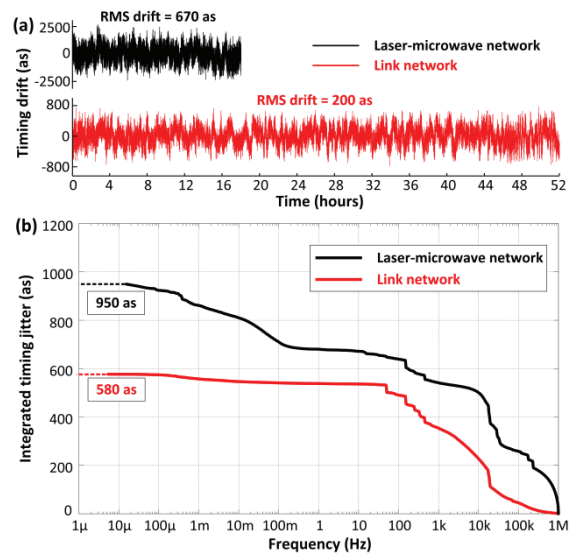


Figure 4: Out-of-loop timing measurement results. (a) Timing drift below 1 Hz and (b) integrated timing jitter.

Stabilization of the timing link network is operated continuously for 52 h and the red curve in Figure 4(a) shows the measured residual timing drift between the two link outputs. The improvements in the timing detection and feedback scheme result in an unprecedented timing error of only 200 as RMS measured by the out-of-loop SH-BOC below 1-Hz offset frequency. The total integrated timing jitter of the link network from 6 μ Hz to 1 MHz is only 580 as (Figure 4(b), red curve), corresponding to a relative timing instability of 3.1×10^{-21} . The majority of the timing jitter stems from the offset frequencies larger than 1 kHz (i.e., ~ 500 as for [1 kHz - 1 MHz]) whereas the noise sources within the locking bandwidth of the link stabilization are effectively suppressed (i.e., only ~ 290 as for [7 μ Hz - 1 kHz]).

After characterizing the link network performance, we activate the remote synchronization of the slave laser and

VCO and observe the out-of-loop timing results with the free-running FSC-BOMPD2. The synchronous laser-microwave network shows an unprecedented long-term precision of 670 as RMS over 18 h (Figure 4(a), black curve). Compared with previous mode-locked laser based timing transfer results [20], this setup includes ten-times longer fiber links and an additional remote microwave synchronization system, yet it still achieves more than an order-of-magnitude improvement. The relative timing stability between the two remotely synchronized devices within the full frequency range from 15 μ Hz to 1 MHz is only 950 as RMS (Figure 4(b), black curve). Excess noise below 100 mHz, is limited by the length fluctuations of the conventional coaxial cables in all RF paths of the FSC-BOMPDs, which can be improved in future work by reducing the electronics into an integrated board or using special phase-stable cables with lower thermal-expansion ratios.

CONCLUSION

The system discussed here represents the first demonstration of a large-scale attosecond-precision laser-microwave network that has the potential of enabling attosecond-precision hard-X-ray photon-science facilities. In turn, this may drive new scientific efforts toward the making of atomic and molecular movies at the attosecond timescale, thereby opening up many new research areas in biology, chemistry, fundamental physics and material science. Besides, this technique will also accelerate developments in many other fields requiring high spatio-temporal resolution such as ultrastable clocks, gravitational wave detection and coherent optical antenna arrays.

REFERENCES

- [1] A. Wootten and A. R. Thompson, "The Atacama Large Millimeter/Submillimeter Array", *Proceedings of the IEEE*, vol. 97, no. 8, pp. 1463-1471, 2009.
- [2] H. Schuhla and D. Behrend, "VLBI: A fascinating technique for geodesy and astrometry", *Journal of Geodynamics*, vol. 61, pp. 68-80, 2012.
- [3] D. H. Bilderback, P. Elleaume and E. Weckert, "Review of third and next generation synchrotron light sources", *J. Phys. B: At. Mol. Opt. Phys.*, vol. 38 pp. S773-S797, 2005.
- [4] B. P. Abbott *et al.*, "LIGO: The Laser Interferometer Gravitational-Wave Observatory," *Rep. Prog. Phys.*, vol. 72, no. 076901, pp. 1-25, 2009.
- [5] P. Emma *et al.*, "First lasing and operation of an angstrom-wavelength free-electron laser", *Nat. Photonics*, vol. 4, pp. 641-647, 2010.
- [6] G. Mourou and T. Tajima, "The Extreme Light Infrastructure: Optics' Next Horizon", *Optics & Photonics News*, vol. 22, pp. 47-51, 2011.
- [7] J. Ulrich, A. Rudenko, and R. Moshhammer, "Free-electron lasers: new avenues in molecular physics and photochemistry", *Annu. Rev. Phys. Chem.*, vol. 63, pp. 635-660 (2012).
- [8] E. Prat and S. Reiche, "Simple Method to Generate Terawatt-Attosecond X-Ray Free-Electron-Laser Pulses", *Phys. Rev. Lett.*, vol. 114, pp. 244801, 2015.
- [9] R. Wilcox, J. M. Byrd, L. Doolittle, G. Huang, and J. W. Staples, "Stable transmission of radio frequency signals on fiber links using interferometric delay sensing", *Opt. Lett.*, vol. 34, no. 20, pp. 3050-3052, 2009.
- [10] M. Glowina *et al.*, "Time-resolved pump-probe experiments at the LCLS", *Opt. Express*, vol. 18, pp. 17620-17630, 2010.
- [11] J. Kim, J. A. Cox, J. Chen, and F. X. Kärtner, "Drift-free femtosecond timing synchronization of remote optical and microwave sources", *Nature Photon.*, vol. 2, pp. 733-736, 2008.
- [12] T. R. Schibli *et al.*, "Attosecond active synchronization of passively mode-locked lasers by balanced cross correlation", *Opt. Lett.*, vol. 28, pp. 947-949, 2003.
- [13] P. T. Callahan, K. Safak, P. Battle, T. Roberts, and F. X. Kärtner, "Fiber-coupled balanced optical cross-correlator using PPKTP waveguides", *Opt. Express*, vol. 22, pp. 9749-9758, 2014.
- [14] J. Kim, F.X. Kärtner, and F. Ludwig, "Balanced optical-microwave phase detectors for optoelectronic phase-locked loops", *Opt. Lett.*, vol. 31, no. 24, pp. 3659-3661, 2006
- [15] M. Y. Peng, A. Kalaydzhyan, and F. X. Kärtner, "Balanced optical-microwave phase detector for sub-femtosecond optical-RF synchronization", *Opt. Express*, vol. 22, pp. 27102-27111, 2014.
- [16] M.Y. Peng *et al.*, "Long-term stable, sub-femtosecond timing distribution via a 1.2-km polarization-maintaining fiber link: approaching 10- 21 link stability", *Opt. Express*, vol. 21, no. 17, pp. 19982-19989, 2013.
- [17] K. Şafak, M. Xin, P. T. Callahan, M. Y. Peng, and F. X. Kärtner, "All fiber-coupled, long-term stable timing distribution for free-electron lasers with few-femtosecond jitter", *Struct. Dyn.*, vol. 2, pp. 041715, 2015.
- [18] M. Xin, K. Şafak, M. Y. Peng, P. T. Callahan, and F. X. Kärtner, "One-femtosecond, long-term stable remote laser synchronization over a 3.5-km fiber link," *Opt. Express* 22, 14904-14912, 2014.
- [19] M. Xin *et al.*, "Attosecond precision multi-km laser-microwave network", *Light Sci. Appl.*, vol. 6, pp. e16187, 2017.
- [20] K. Jung *et al.*, "Frequency comb-based microwave transfer over fiber with 7×10^{-19} instability using fiber-loop optical-microwave phase detectors", *Opt. Lett.*, vol. 39, no. 6, pp. 1577-1580, 2014.